Fluorescence of Europium Tris(bromate) Enneahydrate with Ar^+ Laser Excitation

Masahiko HASUNUMA, Keiko OKADA,* and (the late) Yoshifumi KATO
Department of Chemistry, Faculty of Science, Kobe University, Nada-ku, Kobe 657
(Received January 9, 1984)

The (f,f^*) transitions of europium tris(bromate) enneahydrate crystal between 12000 and 20000 cm^{-1} were measured at 95 K by laser-excited fluorescence spectroscopy. The crystal field components of the ground ($^7F_{0,1\cdots6}$) and the excited states ($^5D_{0,1}$) participating in the transitions were analyzed in terms of the tensor-operator method. Besides electric-dipole transitions, a number of magnetic-dipole transitions were detected in compliance with the selection rule. The theory could reproduce the observed wavenumbers and intensities both for the σ- and π-transitions. The population ratio of the $^5D_0$ to the $^5D_1$ was estimated to be 14.1 from the intensity calculations and the observed results. The result suggests that mixing of g-orbitals is significant for the forced electric-dipole transitions.

The trivalent europium ion of $4f^6$ electronic configuration has a ground ^7F multiplet with a width of about 5000 cm^{-1} and the next low energy levels of ^5D multiplet about 17000—24000 cm^{-1} above. The Eu^{3+} ion in crystals displays characteristic emission in the visible region which arises from the (f,f^*) transitions between these states. In the last decade, a considerable number of studies have been made on the fluorescence of Eu^{3+} doped in a variety of host lattices. So far, however, no work has been reported on the electronic structure of europium tris(bromate) enneahydrate crystals of $Eu(BrO_3)_3\cdot9H_2O$, which has a typical coordination structure of $[Eu(OH_2)_9]^{3+}$. In a previous work,[1] the fluorescence spectrum excited by an Ar^+ laser on the europium tris(ethyl sulfate) enneahydrate crystal (Eu(ES)) was studied. In this structure the Eu^{3+} ion is in the C_{3h} crystal field of $[Eu(OH_2)_9]^{3+}$. Besides the confirmation of the crystal field splittings of the ground ^7F multiplet and the excited $^5D_0$ and $^5D_1$ states, a successful interpretation of the spectral intensities was made by applying the Judd-Ofelt theory.[2,3]

The present study is concerned with the electronic structure of $Eu(BrO_3)_3\cdot9H_2O$ obtained by analysing the laser-excited fluorescence spectra. In this host, the Eu^{3+} ion is in the D_{3h} crystal field of $[Eu(OH_2)_9]^{3+}$ according to X-ray crystallography.[4,5] The transition probabilities for both the electric-dipole (ED) and magnetic-dipole (MD) transitions were also calculated by using the tensor-operator method. Some discussions are given of the calculated and observed relative intensities.

Experimental

Single crystals of $La(BrO_3)_3\cdot9H_2O$ and $Eu(BrO_3)_3\cdot9H_2O$ were prepared by the method described in a previous paper.[6] The fluorescence spectra of the crystals were measured through an analyser to obtain polarization of the emitted radiations whose polarizing planes are perpendicular (σ-) and parallel (π-spectrum) to the principal axis of the crystal. The experimental procedure was the same as in our previous report.[1]

Results and Discussion

Selection Rules. In view of the X-ray crystallographic studies,[4,5] it may appear adequate to assume the D_{3h} crystal field of $[Eu(OH_2)_9]^{3+}$. However, D_3 symmetry was adopted for the theoretical calculations, since it is convenient for the spectral assignments. The crystal field mixes the states which differ in J and J_z, whereupon J and J_z cease to be good quantum numbers. Then the crystal quantum number μ is used to classify the crystal field energy levels. The classification of the crystal quantum number for different

Table 1. Basis functions for the irreducible representations of D_3 symmetry

J	Crystal quantum number μ		
	0^+ (A_1)	0^- (A_2)	±1 (E)
0	$\|0,0\rangle$		
1		$\|1,0\rangle$	$\|1,\pm1\rangle$
2	$\|2,0\rangle$		$\|2,\pm1\rangle$ $\|2,\mp2\rangle$
3	$\frac{1}{\sqrt{2}}(\|3,3\rangle-\|3,-3\rangle)$	$\|3,0\rangle$ $\frac{1}{\sqrt{2}}(\|3,3\rangle+\|3,-3\rangle)$	$\|3,\pm1\rangle$ $\|3,\mp2\rangle$
4	$\|4,0\rangle$ $\frac{1}{\sqrt{2}}(\|4,3\rangle+\|4,-3\rangle)$	$\frac{1}{\sqrt{2}}(\|4,3\rangle-\|4,-3\rangle)$	$\|4,\pm1\rangle$ $\|4,\mp2\rangle$ $\|4,\pm4\rangle$
5	$\frac{1}{\sqrt{2}}(\|5,3\rangle-\|5,-3\rangle)$	$\|5,0\rangle$ $\frac{1}{\sqrt{2}}(\|5,3\rangle+\|5,-3\rangle)$	$\|5,\pm1\rangle$ $\|5,\mp2\rangle$ $\|5,\pm4\rangle$ $\|5,\mp5\rangle$
6	$\|6,0\rangle$ $\frac{1}{\sqrt{2}}(\|6,3\rangle+\|6,-3\rangle)$ $\frac{1}{\sqrt{2}}(\|6,6\rangle+\|6,-6\rangle)$	$\frac{1}{\sqrt{2}}(\|6,3\rangle-\|6,-3\rangle)$ $\frac{1}{\sqrt{2}}(\|6,6\rangle-\|6,-6\rangle)$	$\|6,\pm1\rangle$ $\|6,\mp2\rangle$ $\|6,\pm4\rangle$ $\|6,\mp5\rangle$

Table 2. Selection rules for D_3 symmetry in the case of an even number of electrons

(ED transition)				(MD transition)			
	μ				μ		
μ	0^+	0^-	±1	μ	0^+	0^-	±1
0^+	—	π	σ	0^+	—	σ	π
0^-	π	—	σ	0^-	σ	—	π
±1	σ	σ	σ,π	±1	π	π	σ,π

$|J,J_z>$ states are given for D_3 symmetry in Table 1.[7] The selection rules in terms of the crystal quantum number μ for ED and MD transitions are shown in Table 2.[8]

Spectra. The fluorescence spectra of $Eu(BrO_3)_3 \cdot 9H_2O$ at 95 K excited by a 457.9 nm line of an Ar^+ laser are shown in Figs. 1 and 2. The Raman lines of the vibrational modes were distinguished from the fluorescence lines by reference to the spectrum of $La(BrO_3)_3 \cdot 9H_2O$, which is isomorphous with $Eu(BrO_3)_3 \cdot 9H_2O$ and gives no (f,f^*) transitions, since it has no f-electron in the ground configuration. The σ- and π-polarized spectra exhibit fluorescence lines at the same wavenumbers but with different relative intensities. The intensities were measured by the areas under the curves of the spectra. The lines were assigned to ED and MD transitions between "crystal field levels" on the basis of the selection rules and the calculated transition energies and intensities. The observed wavenumbers and relative intensities of the fluorescence lines of $Eu(BrO_3)_3 \cdot 9H_2O$ are listed in Table 3. Eight strong MD transitions are allowed according to the selection rules for the "ion levels" (*i.e.* $|\Delta J| \leqq 1$) and 12 weak MD transitions are forbidden transitions with $|\Delta J|>1$. While the former strong transitions were already reported by Hellwege,[9] Axe,[10] and Sayre and Freed[11] for Eu(ES), the latter weak transitions were first observed in our previous research applying the laser as a light source.[1] The forbidden transitions occur when there exists a considerable interaction of the free ion with the crystal field, that is, when the influence of J-mixing is appreciable. Table 4 summarizes the crystal field levels of $Eu(BrO_3)_3 \cdot 9H_2O$ determined by the present analysis.

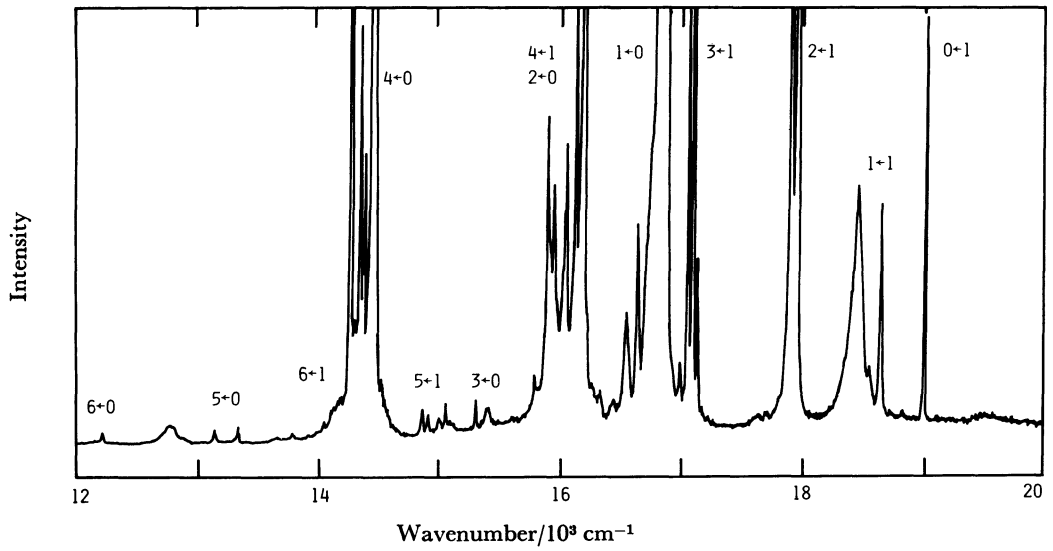

Fig. 1. σ-polarized fluorescence spectra of $Eu(BrO_3)_3 \cdot 9H_2O$ at 95 K excited by the 457.9 nm line of Ar^+ laser. Fluorescence lines assigned to the transitions between the ground ($^7F_{J'}$) and excited substates (^5D_J) are shown as ($J' \leftarrow J$).

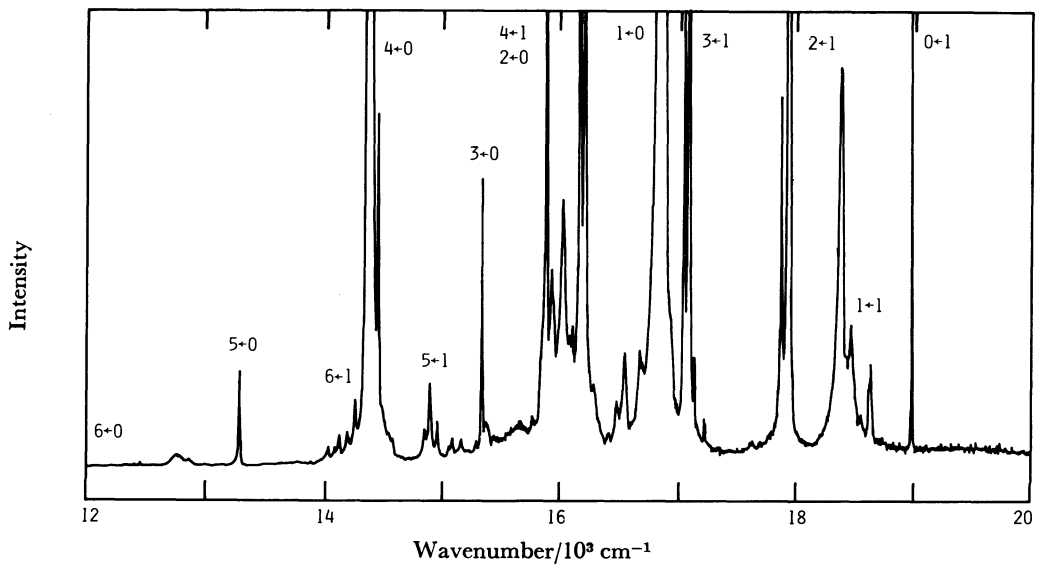

Fig. 2. π-polarized fluorescence spectra of $Eu(BrO_3)_3 \cdot 9H_2O$. Notations are the same as in Fig. 1.

Table 3. Assignments of the fluorescence spectra of $Eu(BrO_3)_3 \cdot 9H_2O$

	$5D_0(0^+)$			$5D_1(\pm1)$			$^5D_1(0^-)$			Averaged energy /cm^{-1}
	σ[b]/cm^{-1}	I_r[c]	Energy[d] /cm^{-1}	σ/cm^{-1}	I_r	Energy /cm^{-1}	σ/cm^{-1}	I_r	Energy /cm^{-1}	
$^7F_0(0^+)$				*19012.2π	1.00	0.0	*19019.7σ	0.81	0.0	0.0±0.2
$^7F_1(\pm1)$	*16900.6π	25.1	352.2	18658.9σ	0.24	352.3	*18666.0π	0.02	353.8	352.7±1.1
(0^-)	*16846.6σ	17.5	404.8							404.8
$^7F_2(\pm2)$	16229.4σ	4.51	1023.4	17986.2π	3.20	1024.8	17995.2σ	0.15	1024.3	1024.2±0.6
(±1)	*16215.0π	1.52	1038.0	17974.0σ	3.41	1037.0	*17982.5π	3.60	1037.1	1037.5±0.5
(0^+)				*17928.0π	0.52	1083.0	*17934.8σ	2.12	1084.0	1083.5±0.5
$^7F_3(3^+)$	15410.7π	2.85	1842.1	17168.1σ	0.95	1842.7				1842.4±0.4
(0^-)				*17128.4π	0.01	1882.4				1882.4
(±2)	15363.0σ	0.08	1889.7	17120.5π	7.81	1890.2	17128.4σ	3.10	1891.0	1890.4±0.7
(±1)	*15335.0π	0.13	1917.7	17092.8σ	2·09	1918.0	*17101.5π	0.12	1918.0	1917.9±0.2
(3^-)				17077.3σ	0.60	1933.8	17085.4π	1.51	1933.9	1933.8±0.1
$^7F_4(\pm2)$	14504.0σ	70.5	2748.5	16260.8π	4.93	2749.8				2749.2±0.7
(3^+)	14440.1π	103.	2812.5	16198.2σ	2.91	2812.3				2812.4±0.1
(±1)	*14407.0π	0.24	2845.5	16163.8σ	3.12	2846.5	*16172.6π	0.04	2845.9	2845.9±0.5
(0^+)				*16103.3π	0.51	2911.2				2911.2
(±2)	14324.4σ	22.5	2928.1	16083.4π	3.22	2927.1	16089.6σ	1.83	2929.5	2928.2±1.3
(3^-)				15936.5σ	1.21	3074.1	15944.2π	3.92	3074.9	3074.5±0.4
$^7F_5(\pm2)$	13408.7σ	0.61	3843.5	15165.8π	0.12	3844.2	15174.4σ	0.11	3843.8	3843.8±0.4
(0^-)	*13402.0σ	0.05	3850.2							3850.2
(±1)				15150.1σ	0.04	3860.1	15158.3π	0.04	3859.9	3860.1±0.1
(3^+)	13371.9π	1.51	3880.3	15128.7σ	0.36	3881.4				3880.8±0.6
(±1)	*13273.6π	0.10	3978.7	15031.3σ	0.01	3978.9				3978.8±0.1
(±2)	13215.0σ	1.21	4037.1	14972.4π	0.97	4037.7	14979.3σ	0.27	4039.4	4037.6±1.8
(3^-)				14932.0σ	0.52	4078.1	14939.6π	0.28	4079.1	4078.6±0.5
$^7F_6(3^+)$	12324.4π	1.80	4927.5	14082.0σ	0.15	4927.9				4927.9±0.5
(±2)	12308.5σ	4.05	4943.4	14067.0π	0.01	4943.0				4943.2±0.2
(±1)				14030.5σ	0.25	4979.4				4979.4
(0^+)				*14027.0π	0.01	4983.7				4983.7
(3^-)				14018.5σ	0.05	4991.4	14028.9π	0.05	4989.7	4990.5±0.9
(±2)	12248.9σ	1.01	5002.9							5002.9
(±1)				13959.5σ	0.05	5050.3				5050.3
(0^+)				*13900.2π	0.02	5109.6				5109.6
(0^-)	*12140.0σ	0.28	5111.8							5111.8

a) The lines with asterisk are due to MD transitions. b) Transition energies in air. c) Relative intensity in case of the intensity of the $^7F_0(0) \leftarrow {}^5D_1(0)$ transition being taken as 1.00. d) Energies of levels in vacuum.

Energy Levels. The procedure for calculating the energies of the 4*f*-orbitals in $[Eu(OH_2)_9]^{3+}$ will be briefly described here. In the case of strong spin-orbit interactions, the wavefunctions for the electrons of the free ion can be written as

$$|\phi) = \sum_n C_n |f^N : qSLJ), \quad (1)$$

where q is an additional quantum number specifying the state. In the presence of the crystal field, the wavefunctions should be rewritten as

$$|\psi_a) = \sum_i a_i |f^N : qSLJM). \quad (2)$$

In taking the summation, a basis set was restricted to the 64 states strongly interacting with ^5D_J and ^7F_J, that is, ^7F_J, $3(^5D_J)$, $2(^5F_J)$, $3(^5G_J)$, ^5H_J, $6(^3P_J)$, ^3D_J, ^3F_J, and ^3H_J states, where the numbers in front of the parentheses are the numbers of states with different q in Eqs. 1 and 2.[12]

The total Hamiltonian of a rare earth ion placed in a crystal field may be written as

$$H = H_{ion} + H_{cry}, \quad (3)$$

where H_{ion} is the Hamiltonian of the free ion and H_{cry} is the potential term provided by the crystal environment around the ions of interest. H_{ion} can be split into

$$H_{ion} = H_0 + H_{es} + H_{so}, \quad (4)$$

where H_0 is the sum of the kinetic energy and the potential energy due to the field of all the inner shell electrons and the nucleus, H_{es} is the electrostatic repulsive potential due to the coulomb and exchange interactions between pairs of the outer shell electrons, and H_{so} is the spin-orbit interaction. H_0 contributes only to a common energy shift for all the levels of a given configuration. Hence the energy levels of the $4f^6$ configuration can be evaluated by diagonalizing the interaction matrix elements of $H_{es}+H_{so}+H_{cry}$. The electrostatic interaction and the spin-orbit interaction can be expressed by a linear combination of the terms of the

Slater radial integrals F_n (n=2, 4, 6) and the spin-orbit coupling constant ζ_{4f}, respectively. The scalar two-body electrostatic interactions arising from the second-order perturbation energies were next considered. They give an additional term to H_{ion} with three configuration interaction (CI) parameters α, β, and γ.[8] The crystal field potential for D_3 symmetry may be expanded in terms of the tensor operator $C_n^{(k)}$ to give in which B_n^k is a

$$H_{cry} = B_0^2C_0^2 + B_0^4C_0^4 + B_3^4(C_3^4+C_{-3}^4) + B_0^6C_0^6 + B_3^6(C_3^6+C_{-3}^6) + B_6^6(C_6^6+C_{-6}^6), \quad (5)$$

crystal field parameter to be determined. First, the matrix concerned with the free ion part was diagonalized by fitting the calculated ion levels to the experimental centers of gravity of the J-manifolds. Next, the crystal field parameters were determined to reproduce the observed crystal field levels for each ion level. Finally, the matrix as a whole was diagonalized by readjusting all the parameters. Table 5 lists the optimum parameters thus obtained. The calculated eigenvalues are in close agreement with the observed ones within root mean square (rms) deviations of 24.0 cm^{-1} and 5.6 cm^{-1} for ion levels and crystal field levels, respectively.

The wavefunctions thus obtained were used to calculate the transition probabilities between crystal field levels.

Intensities. The intensity of radiation for the $\psi_b \leftarrow \psi_a$ transition is given by

$$I(\psi_a : \psi_b) \propto \sigma^4 g(\psi_a) N(\psi_a) [|(\psi_a|\boldsymbol{D}_e|\psi_b)|^2 + |(\psi_a|\boldsymbol{D}_m|\psi_b)|^2]/(2J+1), \quad (6)$$

where σ is the transition energy in wavenumber, $g(\psi_a)$ and $N(\psi_a)$ are the degeneracy and the population of the initial state ψ_a, and $\boldsymbol{D}_e$ and $\boldsymbol{D}_m$ are the ED and MD operators, respectively. The ED operator is written as

Table 4. Observed crystal field levels in $Eu(BrO_3)_3 \cdot 9H_2O$

Level		μ	Energy/cm^{-1}
$^7F_0$	0+	(A_1)	0.0±0.2
$^7F_1$	±1	(E)	352.7±1.1
	0−	(A_2)	404.8
$^7F_2$	±2	(E)	1024.2±0.6
	±1	(E)	1037.5±0.5
	0+	(A_1)	1083.5±0.5
$^7F_3$	3+	(A_2)	1842.4±0.4
	0−	(A_2)	1882.4
	±2	(E)	1890.4±0.7
	±1	(E)	1917.9±0.2
	3−	(A_1)	1933.8±0.1
$^7F_4$	±2	(E)	2749.2±0.7
	3+	(A_2)	2812.4±0.1
	±1	(E)	2845.9±0.5
	0+	(A_1)	2911.2
	±2	(E)	2928.2±1.3
	3−	(A_1)	3074.5±0.4
$^7F_5$	±2	(E)	3843.8±0.4
	0−	(A_2)	3850.3
	±1	(E)	3860.1
	3+	(A_2)	3880.8±0.6
	±1	(E)	3978.8±0.1
	±2	(E)	4037.6±1.8
	3−	(A_1)	4078.6±0.5
$^7F_6$	3+	(A_2)	4927.9±0.5
	±2	(E)	4943.2±0.2
	±1	(E)	4979.4
	0+	(A_1)	4983.7
	3−	(A_1)	4990.5±0.9
	±2	(E)	5002.9
	±1	(E)	5050.3
	0+	(A_1)	5109.6
	0−	(A_2)	5111.8
$^5D_0$	0+	(A_1)	17248.3
$^5D_1$	±1	(E)	19005.8
	0−	(A_2)	19014.4

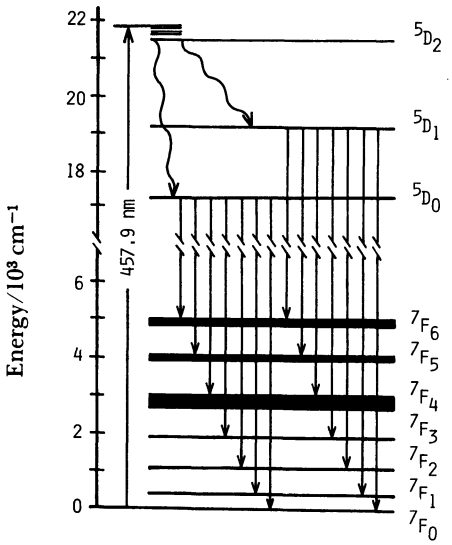

Fig. 3. The energy level diagram of $Eu(BrO_3)_3 \cdot 9H_2O$. Straight and waved arrows indicate the radiative and nonradiative transitions, respectively.

Table 5. Parameter values used in the calculation of energy levels

Parameter/cm^{-1}	
$F2$	179.
$F4$	55.05
$F6$	4.79
ζ_{4f}	1317.
α	49.5
β	998.
γ	995.
$B(2,0)$	202.
$B(4,0)$	−282.
$B(4,3)$	−3.00
$B(6,0)$	−522.
$B(6,3)$	77.
$B(6,6)$	859.
r.m.s. deviation/cm^{-1}	
"ion level"	24.5
"crystal field level"	5.6

$$\boldsymbol{D}_e = -e\sum_i \boldsymbol{r}_i(\mathbf{C}_\rho^{(1)})_i, \tag{7}$$

where $\mathbf{C}_\rho^{(1)}$ is an irreducible tensor of rank 1. The z-component of the ED moment corresponding to the π-polarized emission is obtained with $\rho=0$, and the $(x\pm iy)$-components corresponding to the σ-polarized emission are obtained with $\rho=\pm1$. The ED mechanism of the (f,f^*) transitions has been considered to be of a forced electric dipole origin by Judd[2] and Ofelt.[3] They occur due to the mixing of $nl^{N-1}n'l'$ configurations of opposite parity through the odd terms of the crystal field potential V_{odd}. Then the perturbed state $|\psi_a'\rangle$ is expressed as

$$|\psi_a'\rangle = |\psi_a\rangle - \sum_\eta \left[\frac{(nl^{N-1}n'l':\eta|V_{odd}|\psi_a)}{\Delta E(\eta)}\right]|nl^{N-1}n'l':\eta), \tag{8a}$$

$$\Delta E(\eta) = E(nl^{N-1}n'l':\eta) - E(\psi_a) \simeq \Delta E(n'l'), \tag{8b}$$

where the perturbing potential V_{odd} is defined by

$$V_{odd} = \sum_i \sum_{t,p} A_{tp}\boldsymbol{r}_i^t(\mathbf{C}_p^{(t)})_i. \tag{9}$$

For D_3 symmetry the odd potential has the form

$$V_{odd}(D_3) = \sum_i \sum_t A_{t3}\boldsymbol{r}_i^t(\mathbf{C}_3^{(t)} - \mathbf{C}_{-3}^{(t)})_i. \tag{10}$$

The matrix elements of $\boldsymbol{D}_e$ may be expanded in terms of LS multiplets by the application of the tensor-operator technique to yield

$$\begin{aligned}(\psi_a'|\boldsymbol{D}_e|\psi_b') = {} & \sum_{i,j}\sum_\lambda\sum_{t,p} a_i^* b_j (-1)^{2J+S+L'+\lambda-M+p+\rho}\delta(S,S') \\ & \times (2\lambda+1)[(2J+1)(2J'+1)]^{1/2} \\ & \begin{bmatrix}1 & \lambda & t\\ \rho & -p-\rho & p\end{bmatrix}\begin{bmatrix}J & \lambda & J'\\ -M & P+\rho & M'\end{bmatrix} \\ & \times \begin{Bmatrix}J & J' & \lambda\\ L' & L & S\end{Bmatrix} T_c(t,\lambda)(qSL||\boldsymbol{U}^{(\lambda)}||q'SL'),\end{aligned} \tag{11a}$$

$$\begin{aligned}T_c(t,\lambda) = {} & A_{tp_{l'}}\sum(-1)^{l+l'}2(2l+1)(2l'+1)\begin{bmatrix}l & l & l'\\ 0 & 0 & 0\end{bmatrix}\begin{bmatrix}l & t & l'\\ 0 & 0 & 0\end{bmatrix} \\ & \times \begin{Bmatrix}1 & \lambda & t\\ l & l' & l\end{Bmatrix}(R_{nl}|r|R_{n'l'})(R_{n'l'}|r^t|R_{nl})/\Delta E(\eta),\end{aligned} \tag{11b}$$

where A_{tp} is a perturbing crystal field parameter. From the triangular condition for n-j symbols with $l=3$, Eq. 11 has nonzero matrix elements only if

$$\lambda = 2,\ 4,\ 6,\quad t = \lambda\pm1,\quad l' = 2,\ 4. \tag{12}$$

Therefore, the five parameters $T_c(3,2)$, $T_c(3,4)$, $T_c(5,4)$, $T_c(5,6)$, and $T_c(7,6)$ are required. The $T_c(t,\lambda)$ contains theoretically undeterminable factors by the present method, namely, the crystal field parameter A_{tp}, the radial wavefunction and the energy of the $n'l'$ orbital. Hence, an alternative parametrization proposed by Axe[10] was adopted; this is appropriate to describe the relative intensities of transitions between the crystal field levels by taking the $T_c(t,\lambda)$ as adjustable parameters. A line strength[13] for transitions between ion levels was defined by Judd-Axe[2,10] as

$$S(\phi_nJ:\phi_mJ') = \sum_t\sum_\lambda (2\lambda+1)T_i(t,\lambda)^2|(\phi_nJ|\boldsymbol{U}^{(\lambda)}|\phi_mJ')|^2/(2t+1). \tag{13}$$

The $T_i(t,\lambda)$ is a parameter concerned with the transition between ion levels and should be distinguished from $T_c(t,\lambda)$ for the crystal field levels. The matrix elements of the unit tensor of rank λ can be calculated using the eigenvectors in Eq. 1:

$$\begin{aligned}(\phi_nJ|\boldsymbol{U}^{(\lambda)}|\phi_mJ') = {} & \sum_{n,m} c_n^* c_m \delta(S,S')(-1)^{S+L'+J-\lambda} \\ & \times [(2J+1)(2J'+1)]^{1/2} \\ & \times \begin{Bmatrix}J & J' & \lambda\\ L' & L & S\end{Bmatrix}(f^N:qSL||\boldsymbol{U}^{(\lambda)}||f^N:q'SL').\end{aligned} \tag{14}$$

Consequentry, the parameters $T_i(t,\lambda)$ may be estimated from the observed line strengths using Eq. 13:

$$\begin{aligned}&T_i(3,2) = \pm0.58,\quad T_i(3,4) = \pm0.20,\quad T_i(5,4) = \pm2.39,\\ &T_i(5,6) = \pm0.05,\quad T_i(7,6) = \pm1.46.\end{aligned} \tag{15}$$

An MD transition within the $4f^N$ configuration is allowed since an MD operator $\boldsymbol{D}_m$ is of even parity having the form

$$\begin{aligned}\boldsymbol{D}_m &= -\beta(2S+L),\\ \beta &= -e\hbar/(4\pi mc).\end{aligned} \tag{16}$$

The matrix element of $\boldsymbol{D}_m$ reduces to

$$\begin{aligned}(\psi_a|(\boldsymbol{D}_m)_\rho|\psi_b) = {} & \sum_{i,j} a_i^* b_j (-1)^{J-M}\begin{bmatrix}J & 1 & J'\\ -M & \rho & M'\end{bmatrix} \\ & \times (f^N:qSLJ||\boldsymbol{D}_m||f^N:q'S'L'J'),\end{aligned} \tag{17}$$

where $\rho=0$ and ±1 correspond to σ- and π-polarized radiations, respectively, contrary to ED transitions. According to Condon and Shortley,[13] the matrix elements are nonzero only when they are diagonal in the quantum numbers q, S, and L, and furthermore J satisfies the following three cases ($\Delta J=0,\pm1$):

1) $J'=J$,

$$(qSLJ||\boldsymbol{D}_m||qSLJ') = g[J(J+1)(2J+1)]^{1/2}, \tag{18}$$

where

$$q = 1 + [J(J+1) + S(S+1) - L(L-1)]/[2J+1].$$

2) $J' = J-1$,

$$(qSLJ||\boldsymbol{D}_m||qSLJ') = \left[\frac{(S+L+J+1)(S+L+1-J)(J+S-L)(J+L-S)}{4J}\right]^{1/2}. \tag{19}$$

3) $J' = J+1$,

$$(qSLJ||\boldsymbol{D}_m||qSLJ') = \left[\frac{(S+L+J+2)(S+J+1-L)(L+J+1-S)(S+L-J)}{4(J+1)}\right]^{1/2}. \tag{20}$$

Thus, the MD transition probability can be evaluated straightforwardly by using Eqs. 1 and 2 for ion levels and crystal field levels, respectively.

The calculated values of the relative line strengths are contrasted with the observed ones in Table 6. The comparison enables us to estimate the population of the initial levels by Eq. 6. The two components of the $^5D_1$ state, $^5D_1(0)$ and $^5D_1(\pm1)$, were assumed to be equal in population since they are separated by only 8.6 cm^{-1}. On the other hand, the $^5D_0(0)$ state lies about 1750 cm^{-1}

Table 6. Comparison of the calculated and observed line strength of $^7F_{J'} \leftarrow {}^5D_J$ transitions in $Eu(BrO_3)_3 \cdot 9H_2O$

Upper state	S_{obsd}		S_{theo}	
Lower state	$^5D_0$	$^5D_1$	$^5D_0$	$^5D_1$
$^7F_0$				
$^7F_1$		0.62		$1.86T_1(3,2)^2$
$^7F_2$	14.0		$3.01T_1(3,2)^2$	$0.56T_1(3,2)^2$
$^7F_3$	3.15	19.6		$4.68T_1(3,2)^2+7.88T_1(3,4)^2+5.02T_1(5,4)^2$
$^7F_4$	260.0	21.4	$9.84T_1(3,4)^2+6.26T_1(5,4)^2$	$12.3T_1(3,4)^2+7.84T_1(5,4)^2$
$^7F_5$	4.63	4.18		$4.32T_1(3,4)^2+2.75T_1(5,4)^2+0.15T_1(5,6)^2+0.11T_1(7,6)^2$
$^7F_6$	11.7	1.07	$0.60T_1(5,6)^2+0.45T_1(7,6)^2$	$0.69T_1(5,6)^2+0.50T_1(7,6)^2$

Table 7. Comparison of the theoretical and observed transition intensities of the fluorescence spectra of $Eu(BrO_3)_3 \cdot 9H_2O$

Upper state	$^5D_0(0^+)$			$^5D_1(\pm1)$			$^5D_1(0^-)$		
Lower state	theo. ED	theo. MD	obsd	theo. ED	theo. MD	obsd	theo. ED	theo. MD	obsd
$^7F_0(0^+)$					1.59	1.00		1.28	0.81
$^7F_1(\pm1)$		1.21	1.78	0.38		0.24		0.02	0.02
(0^-)		0.78	1.24						
$^7F_2(\pm2)$	0.24		0.32	0.07	3.19	3.20	0.15		0.15
(±1)		0.11	0.11	0.02	3.35	3.40		3.62	3.60
(0^+)					0.51	0.51		2.40	2.12
$^7F_3(3^+)$	~0		0.20	0.89		0.95			
(0^-)		~0			~0	0.005			
(±2)	~0			7.85	0.02	7.81	4.71		3.10
(±1)		0.08	0.01	1.21	0.02	2.09		0.34	0.12
(3^-)				0.90		0.60	0.54		1.51
$^7F_4(\pm2)$	4.75		5.00	4.54	0.01	4.93	~0		
(3^+)	6.15		7.30	2.28		2.91			
(±1)		0.02	0.02	4.53	~0	3.12		0.03	0.04
(0^+)					~0	0.51		~0	
(±2)	1.65		1.57	5.71	~0	3.22	2.16		1.83
(3^-)				2.27		1.21	2.90		3.92
$^7F_5(\pm2)$	0.02		0.04	0.17	~0	0.12	0.25		0.11
(0^-)		0.006	0.004		~0				
(±1)		~0		0.65	~0	0.10	0.02	~0	0.04
(3^+)	0.05		0.11	0.55		0.36			
(±1)		0.03	0.007	0.20	~0	0.01		~0	
(±2)	0.01		0.08	0.37	~0	0.97	1.02		0.52
(3^-)				0.92		0.52	0.66		0.81
$^7F_6(3^+)$	0.01		0.13	0.03		0.15			
(±2)	0.02		0.28	0.06		0.01	~0		
(±1)		~0		0.26	~0	0.25		~0	
(0^+)					0.01	0.01		~0	
(3^-)				0.06		0.05	0.03		0.05
(±2)	0.04		0.07	~0	~0		~0		
(±1)		~0		0.02	~0	0.05		~0	
(0^+)				~0	0.02	0.02		~0	
(0^-)		0.02	0.02		~0				

below the $^5D_1$ state. The ratio of the population of $^5D_0$ to that of $^5D_1$ is given by

$$\frac{N(^5D_0)}{N(^5D_1)} = \frac{S_{obsd}(^5D_0:{}^7F_J)/S_{calcd}(^5D_0:{}^7F_J)}{S_{obsd}(^5D_1:{}^7F_{J'})/S_{calcd}(^5D_1:{}^7F_{J'})} = R(^5D_0 \rightarrow {}^7F_J:{}^5D_1 \rightarrow {}^7F_{J'}), \quad (21)$$

where $N(^5D_J)$ stands for the sum of populations overall the components of the J-manifold. Since the fluorescence intensity is proportional to the population difference between the initial and the final states, the population ratio can be estimated from the intensities of two transitions involving the same final state. Thus, the population ratio was calculated from the line strengths in Table 6 to be

$$R(^5D_0 \rightarrow {}^7F_2:{}^5D_1 \rightarrow {}^7F_2) = 14.1, \quad (22a)$$

$$R(^5D_0 \rightarrow {}^7F_4:{}^5D_1 \rightarrow {}^7F_4) = 15.5, \quad (22b)$$

$$R(^5D_0 \rightarrow {}^7F_6:{}^5D_1 \rightarrow {}^7F_6) = 12.6. \quad (22c)$$

The average of these values gives 14.1 as the population ratio $^5D_0$ to $^5D_1$. The result differs from the Boltzmann distribution at 77k.

The values of $T_i(t,\lambda)$ of Eq. 15 for free ion levels were revalued for crystal field levels by a least-squares method.

$$T_c(3,2) = 0.25, \quad T_c(3,4) = -0.10, \quad T_c(5,4) = -2.71,$$
$$T_c(5,6) = -0.02, \quad T_c(7,6) = -0.10. \quad (23)$$

The calculated relative intensities are compared with the observed ones in Table 7, where the intensity of the line $^7F_0(0^+) \leftarrow {}^5D_1(\pm 1)$ is taken to be unity. The observation is well reproduced by the calculation.

Since $T_c(t,\lambda)$ is related to the radial wavefunction $R_{n'l'}$, the contribution of the admixing orbital $n'l'$ can be estimated. Then a parameter

$$\Gamma = \sum_{n'} \Omega(n'g)/[\sum_{n'} \Omega(n'g) + \sum_{n'} \Omega(n'd)], \quad (24)$$

proposed by Axe[10] may be introduced, where

$$\Omega(n'l') = (R_{4f}|r|R_{n'l'})(R_{n'l'}|r^t|R_{4f})/\Delta E(n'l'). \quad (25)$$

The parameter Γ may be considered as a kind of measure of the contribution of the admixing orbital $n'l'$, *i.e.*, if only d-orbitals contribute, $\Gamma=0$, and if only g-orbitals contribute, $\Gamma=1$. Approximate ratios between $T_c(t,\lambda)$ values given by Eq. 11b are shown as function of Γ as

$$\frac{T_c(3,4)}{T_c(3,2)} = \frac{1.95-1.42\Gamma}{1.0+1.44\Gamma}, \quad (26a)$$

$$\frac{T_c(5,6)}{T_c(5,4)} = \frac{6.08-6.19\Gamma}{1.0+5.00\Gamma}. \quad (26b)$$

From the $T_c(t,\lambda)$ values in Eq. 23 the value of Γ was calculated to be 0.968 and 0.987 for the $t=3$ (Eq. 26a) and $t=5$ (Eq. 26b), respectively. Consequently, it is concluded that the $n'g$-orbital plays a dominant role in configuration mixing for ED transitions.

This work was partially supported by a Grant-in-Aid for Scientific Research to Y. K. from the Ministry of Education, Science and Culture (No. 58350049).

References

1) T. Ohoka and Y. Kato, *Bull. Chem. Soc. Jpn.*, **56**, 1289 (1983).
2) B. R. Judd, *Phys. Rev.*, **127**, 750 (1962).
3) G. S. Ofelt, *J. Chem. Phys.*, **37**, 511 (1962).
4) L. Helmholz, *J. Am. Chem. Soc.*, **61**, 1544 (1939).
5) S. K. Sikka, *Acta Crystallogr., Sect. A*, **25**, 621 (1969).
6) Y. Kato, K. Okada, H. Fukuzaki, and T. Takenaka, *J. Mol. Struct.*, **49**, 57 (1978).
7) G. H. Dieke, "Spectra and Energy Levels of Rare Earth Ions in Crystals," Interscience Publ., New York (1968).
8) B. G. Wybourne, "Spectroscopic Properties of Rare Earths," Interscience Publ., New York (1965).
9) K. H. Hellwege, U. Johnsen, H. G. Kahle, and G. Schaack, *Z. Phys.*, **148**, 112 (1957).
10) J. D. Axe, Jr., *J. Chem. Phys.*, **39**, 1154 (1963).
11) E. V. Sayre and S. Freed, *J. Chem. Phys.*, **24**, 1213 (1956).
12) C. W. Nielson and G. F. Koster, "Spectroscopic Coefficients for the p^n, d^n, and f^n configurations," M. I. T. Press, Cambridge, Mass. (1964).
13) E. U. Condon and G. H. Shortley, "The Theory of Atomic Spectra," Cambridge Univ. Press, Cambridge, England (1964).